

Shock-Induced Shifts in the Aluminum *K* Photoabsorption Edge

L. DaSilva, A. Ng, B. K. Godwal,^(a) G. Chiu, and F. Cottet^(b)

Physics Department, University of British Columbia, Vancouver, British Columbia, Canada V6T 2A6

M. C. Richardson and P. A. Jaanimagi

Laboratory for Laser Energetics, University of Rochester, Rochester, New York 14627

Y. T. Lee

Lawrence Livermore National Laboratory, University of California, Livermore, California 94550

(Received 25 July 1988)

We present results of studies on shock-induced shifts in the *K* photoabsorption edge of aluminum. Time-resolved x-ray spectroscopic measurements indicated maximum red shifts of ~ 7 eV for compressions of ~ 2.2 times the normal density. The results are interpreted using hydrodynamic simulations which incorporated a new model for calculating the *K*-edge energy in a dense plasma.

PACS numbers: 52.35.Tc, 52.50.Jm, 62.50.+p, 78.70.Dm

In recent years, high-power lasers have been found to have a growing use in research at high pressure and density. In particular, Hugoniot studies have focused on the measurement of shock speed¹⁻⁵ and temperature.⁵ These, however, yielded little information on the ionization state or electronic structure of the dense matter. Most recently, Bradley *et al.*⁶ reported on the first experiment to probe the electronic structure of radiatively-heated and shock-compressed KCl by measuring the photoabsorption edge shift of chlorine in a multilayered target. In this paper, we present measurements of shock-induced shifts in the aluminum *K* edge in laser-irradiated aluminum foils. Aluminum was chosen because its high-pressure equation of state is well established.⁷ The use of a uniform target allows us to follow the change in the *K* edge as the shock pressure is varied during the laser pulse. Most importantly, shock propagation will not be complicated by impedance mismatches between different target layers and the shock can be characterized by transit time measurements. Furthermore, using thick targets and long pulses, we can access shock-compressed aluminum without radiative preheat. A new model for calculating the *K*-edge energy was used in coupled radiation-hydrodynamic simulations to determine the edge shift due to shock compression. The predictions showed good qualitative agreement with the measurements.

In the experiment, aluminum foils were irradiated with a $0.53\text{-}\mu\text{m}$, 2.3-ns (FWHM) laser pulse. For the absorption spectroscopy measurement, $25\text{-}\mu\text{m}$ aluminum targets were chosen so that the shock would reach the target rear surfaces at a time near peak laser intensity. The laser beam was focused onto the target with $f/5$ optics at normal incidence. The intensity distribution at focus approximated a trapezoidal profile with 80% of the laser energy contained in a spot of $\sim 80\text{ }\mu\text{m}$ diam. As the shock wave was observed to emerge from the target-free surface in a region of $\sim 80\text{ }\mu\text{m}$ diam, we considered

the effective irradiance to be the averaged absorbed irradiance in this focal spot region. This was $\sim 2.3 \times 10^{13}$ W/cm². To determine the resulting shock trajectory, shock transit times through $25\text{-}53\text{-}\mu\text{m}$ aluminum foils were measured from observations of luminous emission at target-rear surface. Details of this diagnostic have been described previously.⁵ The results are presented in Fig. 1. These show good agreement with one-dimensional hydrodynamic simulations⁸ which included multi-group radiation transport.⁹ Thus, a good estimate of the pressure and density in the target as a function of time could be made using a known equation of state.¹⁰ The calculated peak shock pressure was 3.5 Mbar which yielded a compression of 2.2.

To determine the *K* edge in the shocked material, x-

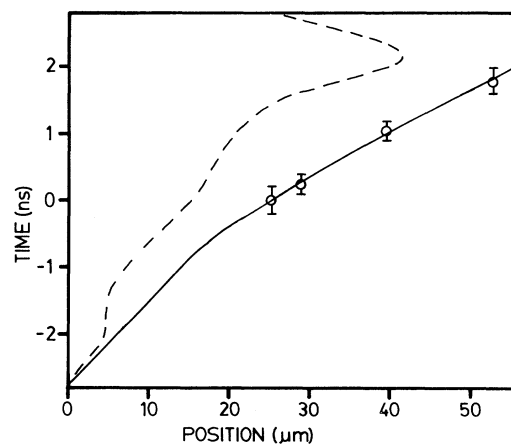


FIG. 1. Laser-driven shock wave in aluminum. Results from transit time measurements (circles) and one-dimensional simulations (solid curve). Also indicated is the calculated trajectory of the target layer giving rise to the most red shifts in the aluminum *K* edge (dashed curve). The zero corresponds to the time of peak laser intensity.

ray emission from the aluminum plasma on the target front side was used to backlight the target. This provided a continuum source in the spectral region (1545–1570 eV) near the aluminum K edge.⁹ More importantly, it eliminated the need for a layered target structure which could modify the shock dynamics due to the impedance mismatches between layers. X rays transmitted through the target at 3° – 7° off target normal were recorded by a streaked spectrograph consisting of a curved (6-in. radius of curvature) penta erythritol (PET) crystal and an x-ray streak camera.¹¹ The crystal was used in a collimating mode to reduce chromatic aberrations. Spectral resolution of this system was 1.5 eV (crystal limited) and the temporal resolution was approximately 20 ps. The location of the crystal directly behind the target precluded simultaneous observation of the shock-induced luminous emission at the target-rear surface.

Figure 2 shows a transmitted x-ray spectrum for a 25- μm target. The spectral dispersion was calibrated using the $K\alpha$ (Al^{8+}) line¹² at 1540 eV and the normal position of the aluminum K edge at 1560 eV. The K edge at normal conditions was determined *in situ* by observing x rays transmitted through a 5- μm target with a 9- μm aluminum foil placed in front of the streak camera. The measured dispersion at the camera cathode was 1.6 eV/mm. The spectra lines observed at late times during target decompression^{13,14} at ~ 1575 and 1580 eV were identified as Al^{10+} satellites. Time zero corresponded to the time of peak laser intensity. This timing reference was obtained by measuring simultaneously the front-side He α ($1s2p-1s^2$) line at 1598 eV and the transmitted satellite line at 1575 eV. The He α emission was correlated with the laser pulse by adopting the ~ 200 -ps delay in the emission peak relative to the laser pulse peak derived from one-dimensional simulations⁷ which incorporated nonlocal-thermodynamic-equilibrium atomic physics.⁸

Because of the limited x-ray emission, the transmitted spectrum could only be recorded on 20000 ASA Polaroid film. Thus, we could not measure its spectral in-

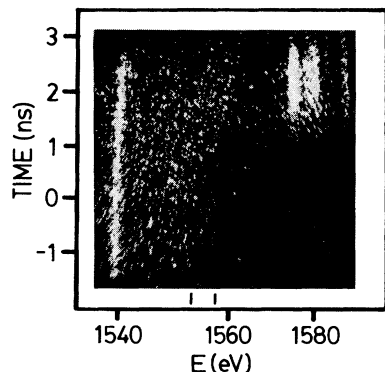


FIG. 2. Single-shot x-ray spectrum transmitted through a 25- μm aluminum target.

tensity. From observations of x rays through aluminum filters placed in front of the streak camera, the dynamic range of the film was estimated to be better than five. Because of insufficient x-ray intensity at the beginning of the laser pulse, the initial unshifted position of the K edge could not be observed. At later times, a clear red shift of the K edge was observed over a relatively long period before the shock reached the target rear surface (near time zero). The edge then shifted back towards its normal position at 1560 eV as the target decompressed.¹³ This red-shift feature of the K edge was highly reproducible. The maximum red shift observed was 7 ± 2 eV. Although we could not obtain a calibrated intensity measurement from the Polaroid film, a semiquantitative assessment of the K -edge profile was made by digitizing a photographic negative of the Polaroid record. An example of the spectrum thus analyzed is presented in Fig. 3. The edge is identified by its "top" and "bottom" positions by A and B , respectively.

To calculate the K -edge energy in shocked aluminum, we considered its average ionization state^{15,16} $\langle Z \rangle$. First, we evaluated the K -shell ionization energy of an isolated aluminum atom with charge $\langle Z \rangle$ based on a Hartree-Fock model.¹⁷ This was then corrected by including the effects of electron degeneracy (ΔE_{deg}) and the effects of neighboring free electrons and ions on the bound energy level (ΔE_{cl}). ΔE_{deg} was given by the sum of the chemical potential of the electron gas and the contribution due to e - e and e - i interactions, which was evaluated using

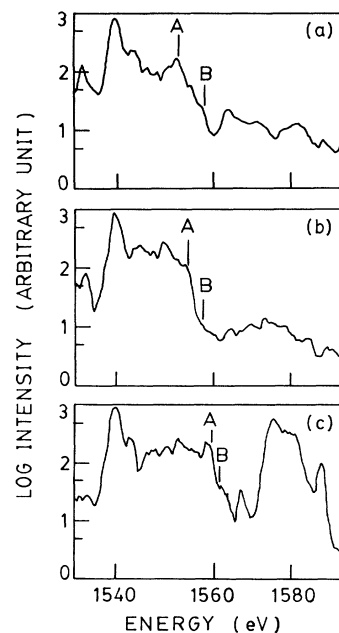


FIG. 3. Single-shot transmitted x-ray spectra at different times obtained from digitizing a photographic negative of the Polaroid record in Fig. 2: (a) -1 to -0.5 ns, (b) 0.5 to 1.0 ns, and (c) 1.5 to 2.0 ns.

the prescription of the second-order pseudopotential theory.¹⁸ ΔE_{cl} was computed from the linearized-muffin-tin-orbital method¹⁹ assuming face-centered-cubic structure and including angular momentum states up to $l=3$. The shift in the bound K level in the dense electron-ion system was approximated by the shift in the energy of an atomic level when it became a band state. For aluminum at normal density and temperature, this model yielded a K edge of 1560.8 eV which compared favorably with the accepted value²⁰ of 1560 eV. The small discrepancy may be an indication of the model accuracy. Figure 4 shows the calculated shift in the K edge along the principal Hugoniot.⁹ Comparable results were obtained from a model similar to that used by Bradley *et al.*,²¹ which differed in the calculation of ΔE_{deg} ²² and ΔE_{cl} .²³ We have also used the HOPE²⁴ and INFERNO²⁵ codes to evaluate the K -edge shift, which treat the electronic structure of the bound and free electrons in a fully self-consistent manner. At twofold shock compression, HOPE yields a red shift of 1.7 eV, while that calculated using INFERNO is less than 0.5 eV. These are much less than the measured value. They also disagree with the calculations using the model presented here and a similar one of Bradley *et al.* These discrepancies are being investigated, and the details will be published later.

Using our model in a one-dimensional, radiation⁹ and hydrodynamic⁸ code, a temporal history of the K -edge energy can be calculated. Because of the time-varying nature of the ablation process, laser-driven shocks are not steady waves particularly during the rising portion of the laser pulse when the ablation pressure is rapidly increasing. Consequently, the state of the shocked target is inhomogeneous. The material behind the shock front

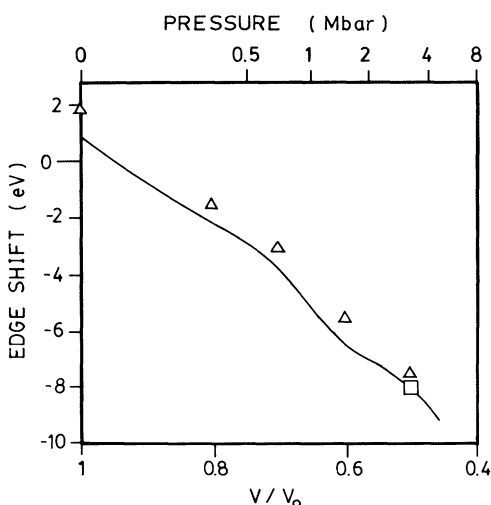


FIG. 4. Shifts in the K photoabsorption edge as a function of shock pressure and compression derived from the present model (solid line) and a model similar to that of Bradley *et al.* (V is the specific volume and V_0 is that under normal conditions).

is compressed more isentropically as it experiences an increasing pressure pulse. On the other hand, radiation transport produces a region of dense material ahead of the ablation zone with temperatures above the Hugoniot values. Fortunately, in the pressure regime of interest, the shift in the K edge is predominantly a density effect. Moreover, the absorption spectroscopy is sensitive to the material causing the most red shift. This is due to the large opacity change (~ 400 vs 4000 cm^2/g) across the K edge, which for a $5\text{-}\mu\text{m}$ region implies 2 orders of magnitude difference in x-ray transmission. The K -edge measurement thus probes the layer of material behind the shock front, where the maximum density occurs (Fig. 1). For a $25\text{-}\mu\text{m}$ target at an absorbed irradiance of $\sim 2.3 \times 10^{13}$ W/cm^2 , the temporal change in the K edge is indicated in Fig. 5 by following the 10% and 90% normalized transmission contours (normalized to peak transmission across the edge). The calculation was made with 0.3-eV resolution but did not include any edge broadening mechanism. Before shock breakout the growing shock pressure causes the K edge to be increasingly red shifted. The small step near -2 ns represents the effect of ionization in the ablation process. As the target decompresses following shock breakout, the K edge begins to shift back towards its normal position. This shows good qualitative agreement with the observation.

To assess the influence of two-dimensional hydrodynamic effects on the experiment, we have performed a ray-tracing calculation in a two-dimensional, fluid code SHYLAC2,²⁶ which has been augmented with the SESAME equation of state. This code did not treat the process of laser-matter interaction. Instead, it assumed an applied pressure pulse on the target-front surface. Using the resulting density profiles, x-ray transmission through the target in various directions could be determined. The transmitted x-ray spectra viewed at 5° (diffraction angle

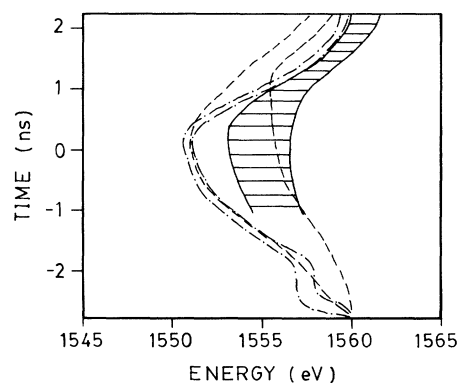


FIG. 5. Temporal evolutions in the aluminum K -edge energy. Results from measurements (hatched area with the upper and lower bounds in the shifts corresponding to the A and B positions in Fig. 3).

for 1560 eV) were calculated for a spatially trapezoidal (80 μm FWHM) and temporal Gaussian (2.3 ns FWHM) pressure pulse with a peak pressure of 3.5 Mbar. The result is included in Fig. 5. The slightly slower shifting of the K edge back towards its normal position (1560 eV) following shock breakout could be attributed to the absence of ablation and radiation transport processes in SHYLAC2. Apparently, two-dimensional effects can cause the edge to appear broadened. Results of this calculation gave better agreement with observation.

We have also observed red shifts in the aluminum K edge in 9- and 16- μm targets. At the time of peak laser intensity, these were 3 ± 2 and 4 ± 2 eV, respectively, which compared favorably with the one-dimensional simulation results of 3 ± 1 and 5 ± 1 eV. The agreement may be fortuitous in view of the unknown two-dimensional effects of shock release at the target-rear side for these thinner targets. The observation nonetheless corroborates our findings in the 25- μm targets.

In conclusion, shock-induced shifts in the aluminum K edge have been measured using a well-characterized shock produced in laser-irradiated foils. The observation showed good qualitative agreement with model predictions. Since calibrated intensity measurements across the absorption edge could not be made, the observations could be interpreted as a broadening of the edge rather than a shift. Lacking any theoretical assessments of the process and effects of broadening, this question remains open. The temporal evolution in the K edge, as indicated in both experiment and simulations, further suggests that it may provide an interesting diagnostic for tracking laser-driven shock compression in an opaque target. The diagnostics may also be viable for inferring shock pressures up to ~ 2 Mbar, where the K -edge energy remains a relatively sensitive function of pressure.

We wish to thank Dr. David Liberman for his enlightening discussions.

^(a)Permanent address: Bhabha Atomic Research Centre, Trombay, Bombay, India.

^(b)Permanent address: Université de Poitiers, rue Guillaume VII, 86034 Poitiers CEDEX, France.

¹L. Vesser and J. Solem, Phys. Rev. Lett. **40**, 1291 (1978).

²R. J. Trainor, J. W. Shaner, J. W. Auerbach, and N. C. Holmes, Phys. Rev. Lett. **42**, 1154 (1979).

³R. J. Trainor, N. C. Holmes, R. A. Anderson, E. M. Campbell, W. C. Mead, R. J. Olness, R. E. Turner, and F. Ze, Appl. Phys. Lett. **43**, 542 (1983).

⁴F. Cottet, J. P. Romain, R. Fabbro, and B. Faral, Phys. Rev. Lett. **52**, 1884 (1984).

⁵A. Ng, D. Parfeniuk, and L. DaSilva, Phys. Rev. Lett. **54**, 2604 (1985).

⁶D. K. Bradley, J. Kilkenny, S. J. Rose, and J. D. Hares, Phys. Rev. Lett. **59**, 2995 (1987).

⁷W. J. Nellis, J. A. Moriarty, A. C. Mitchell, M. Ross, R. G. Dandrea, N. W. Ashcroft, N. C. Holmes, and G. R. Gathers, Phys. Rev. Lett. **60**, 1414 (1988).

⁸P. Celliers, Ph.D. thesis, University of British Columbia, 1988 (unpublished).

⁹D. Duston, R. W. Clark, J. Davis, and J. P. Apruzese, Phys. Rev. A **27**, 1441 (1983).

¹⁰SESAME Data Library, Los Alamos National Laboratory, Table No. 3715.

¹¹P. A. Jaanimagi and B. L. Henke, Bull. Am. Phys. Soc. **28**, 5421 (1983).

¹²This might have been the one-photon, two-electron decay transition at 1535 eV observed by Lunney *et al.* from plasma emissions on target front side [Rutherford Annual Report, 1984 (unpublished), p. A3.9]. If this were true, we would have underestimated the dispersion and hence the observed red shift in the K edge by $\sim 15\%$.

¹³A. Ng, F. P. Adams, Y. Gazit, and L. DaSilva, Phys. Fluids **30**, 186 (1987).

¹⁴F. P. Adams, A. Ng, and Y. Gazit, Rev. Sci. Instrum. **58**, 1130 (1987).

¹⁵C. A. Rouse, Phys. Rev. **176**, 423 (1968).

¹⁶B. K. Godwal, Phys. Rev. A **28**, 1103 (1983).

¹⁷F. Hermann, and S. Skillman, *Atomic Structure Calculations* (Prentice-Hall, New Jersey, 1963), p. 10.

¹⁸V. Heine and D. Weaire, in *Solid State Physics*, edited by F. Seitz, D. Turnbull, and H. Ehrenreich (Academic, New York, 1970), Vol. 24, p. 249.

¹⁹H. L. Skriver, *LMTO Method*, Springer Series in Solid-State Sciences Vol. 41 (Springer-Verlag, Berlin, 1984).

²⁰B. L. Henke, P. Lee, T. J. Tanaka, R. L. Shimabukuro, and B. K. Fujikawa, At. Data Nucl. Data Tables **27**, 1 (1982).

²¹D. K. Bradley, J. D. Hares, A. Rankin, and S. J. Rose, Rutherford Appleton Report No. RAL-85-020, 1985 (unpublished).

²²J. P. Cox, *Principles of Stellar Structure* (Gordon and Breach, New York, 1968), Vol. 1.

²³J. Stewart and K. Pyatt, Astrophys. J. **144**, 1203 (1966).

²⁴B. F. Rozonyai, Phys. Rev. A **5**, 1137 (1972).

²⁵D. A. Liberman, Phys. Rev. B **20**, 4981 (1979); J. Quant. Spectrosc. Radiat. Transfer **27**, 335 (1982).

²⁶L. Marty, Ph.D. thesis, Université de Poitiers, 1988 (unpublished).

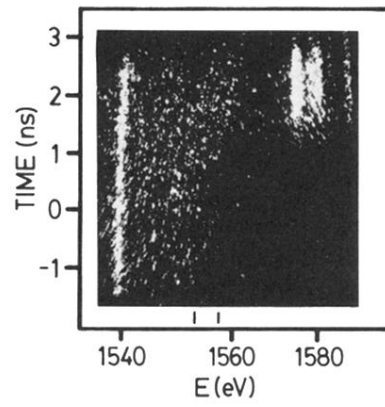


FIG. 2. Single-shot x-ray spectrum transmitted through a 25- μm aluminum target.